Research Article

BIOMEDICAL Journal of Scientific & Technical Research

ISSN: 2574 -1241

DOI: 10.26717/BJSTR.2026.64.010079

Engineering Retro-Proteins Highlights Immunoglobulin-Domain Scaffold Plasticity as a Framework for Therapeutic Discovery

Mason Terry[3], André Hurtado[1], Christopher Mendoza[2], Israel Davila Aleman[1], Amber Gonda[1] and Dario Mizrachi[3]*

[1]*Department of Cell Biology and Physiology, Brigham Young University, Provo, Utah, USA*

[2]*College of Business MBA program, California State University Chico, USA*

[3]*Noorda College of Osteopathic medicine, Provo, Utah, USA*

***Corresponding author:** Dario Mizrachi, Noorda College of Osteopathic Medicine, Provo, Utah, USA. **ORCID ID:** 0000-0002-8586-5905

ARTICLE INFO

Received: January 17, 2026

Published: February 06, 2026

Citation: Mason Terry, André Hurtado, Christopher Mendoza, Israel Davila Aleman and Amber Gonda, Dario Mizrachi. Engineering Retro-Proteins Highlights Immunoglobulin-Domain Scaffold Plasticity as a Framework for Therapeutic Discovery. Biomed J Sci & Tech Res 64(4)-2026. BJSTR. MS.ID.010079.

ABSTRACT

Background: Amino acid sequences of native proteins are generally not palindromic. The protein molecule obtained as a result of reading the amino acid sequence backwards, i.e., a retro-protein, has the same amino acid composition and the same hydrophobicity profile as the native sequence, but may behave as a different molecule.

Methods: R4 is a directed evolution protein product of Scfv-13 that binds β-galactosidase. Additionally, junctional adhesion molecule A (JAMA) is a cell adhesion molecule, an immunoglobulin domain-containing tight junction membrane protein. In this study, we report on the properties of retro-R4 (rR4) and retro-JAMA (rJAMA).

Results: Both retro-proteins examined here retain the function of the parental protein. While rR4 remains a binding protein, its new target is glutamine-fructose-6-phosphate aminotransferase (GLMS), a native *E. coli* protein. rJAMA retains the ability to drive cell-cell interactions but lost its ability to strengthen its binding in the presence of Zinc.

Conclusion: Protein engineering strategies resulting in retro-proteins of immunoglobulin-domain containing proteins may have novel applications that can translate in antibody discovery for therapeutics.

Keywords: Immunoglobulin Domain; Antibody; Cell Adhesion Molecule; Outer Membrane Vesicle; Retro Protein

Abbreviations: AB: Antibody; IgSF: Immunoglobulin Superfamily; Ig: Immunoglobulin; CAMs: Cell Adhesion Molecules; scFv: Single Chain Fragment Variable; HRP: Horseradish Peroxidase; GLMS: Glutamine-Fructose-6-Phosphate Aminotransferase; SEC: Size Exclusion Chromatography; FC: Flow Cytometry; DPBS: Dulbecco's Phosphate-Buffered Saline; SD: Standard Deviation; MBP: Maltose Binding Protein; JAMA: Junctional Adhesion Molecule A; NTA: Nanoparticle Tracking Analysis

Introduction

Proteins are biological macromolecules composed of amino acids. Protein structure is the first obstacle to achieving function [1]. Since the original report by Anfinsen [2] describing the principles that govern the folding of proteins, it is generally accepted that the structure of a protein is determined by its amino acid sequence, as read from the N-terminus to the C-terminus. There is increasing interest in natural and *de novo* designed proteins and peptides as therapeutics [3]. Chief among the protein engineering efforts has been antibody (Ab) design [4]. Abs are proteins that are capable of antigen recognition. The structure of Abs classifies them as members of the immunoglobulin superfamily (IgSF), the largest superfamily of proteins [5,6]. Ab engineering consists of modifying their sequence and/or structure to enhance or decrease their function (Graphical abstract). Monoclonal Abs in particular have revolutionized the fields of diagnosis and immunotherapy for the treatment of a variety of diseases and cancers [7]. However, challenges remain with the production of monoclonal Abs showing high response rates in patients, but low toxicity [4]. Thus, Ab engineering is a major translational challenge that aims to

produce effective monoclonal Abs with optimal processing, stability, and tolerance [8].

All Abs are comprised of paired heavy and light polypeptide chains, and the generic term "immunoglobulin" (Ig) is used for all such proteins [9]. The light chain consists of two Ig domains. Many proteins are partly or entirely composed of Ig domains that were first described in antibody molecules [9].

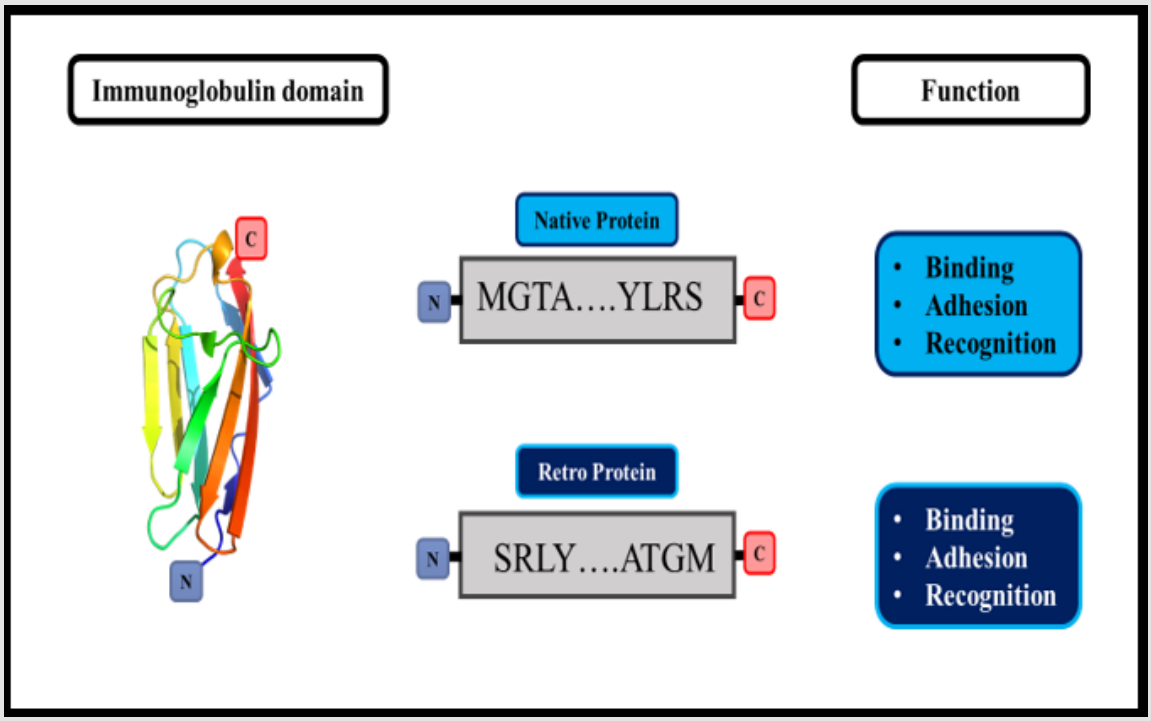

Graphical Abstract.

Ig domains are characteristic of proteins of the IgSF, including Abs, T-cell receptors, MHC molecules, cell adhesion molecules (CAMs), and many others [10]. The Ig domain consists of a sandwich of two β sheets held together by a disulfide bond and termed the Ig fold [10]. The most common Ab format is a single chain fragment variable (scFv) [11]. ScFv contains the complete antigen-binding domain of an intact Ab, with ScFv fragments having important medical applications [12]. Several approaches have been employed to increase the affinity, avidity and structural stability of these Ab fragments [12,13]. Although many strategies have been used so far to engineer ScFv Abs, there has been no attempt to use the retro-protein approach. Ab mimetics represent the fourth generation of Ab engineering, following polyclonal Abs, monoclonal Abs, and genetically engineered Ab fragments [14]. Nevertheless, the development of these molecules has been met with numerous obstacles, suggesting the need for novel strategies [14-16] such as next generation Ab-drug conjugates. However, the increased complexity, multimodal nature, and difficulty in predicting the effects (e.g., anticancer immunity) of these molecules continues to present challenges for their development [17].

During the 1990s, several reports described the consequences of inverting peptides and proteins. Guichard and colleagues [18] described the synthesis of three analogues of the model peptide sequence IRGERA, corresponding to the COOH-terminal residues 130-135 of histone H3.

The retro-inverso peptide IRGERA mimicked the structure and antigenic activity of the natural L-peptide [18]. When Abs were raised against these variants, large differences in K_a values were observed when each monoclonal Ab was tested with respect to the other peptides [18]. Furthermore, antigenicity and immunogenicity can be achieved by retro-inverso isomers of natural antigenic peptides. Hybrid peptides derived from cercropin A and melittin maintain antimicrobial activity when prepared as retro-inverso forms [19]. Other examples of retro-peptides or retro-proteins exist, but are still rare [20-22].

Although inverted sequences are occasionally found in genomic DNA, no native retro-protein has yet been reported. A retro-protein results from reading the coding sequence backwards, or in the opposite sense. It has the same amino acid composition and hydrophobicity profile as the native sequence. However, since these proteins are not native, an obvious question is whether retro-proteins fold into well-defined, native-like structures similar to those of natural

proteins. Furthermore, do retro-proteins have similar function to the native protein? Retro-proteins are dissimilar to the original sequence, despite their common hydrophobic and hydrophilic pattern, amino acid composition, and consequent tertiary contacts. Recent progress in the prediction of protein folding [23] has extended our understanding of the protein folding space. Nevertheless, these advances cannot yet be used to predict protein function.

For this research, we have elected to study two members of the IgSF, one with cell adhesive properties and the other with recognition capabilities. Each was converted to retro-inverted forms, and their function subsequently analyzed. ScFv-13 is a human Ab fragment specific for β-galactosidase (β-gal) [24] and categorized as an antigen recognition molecule. This fragment has been subjected to directed evolution strategies *in vivo*, resulting in scFv-13. R4 (thereafter referred to as R4), a mutant version with high affinity for β-gal and greater solubility [25]. The second member of the IgSF studied here was a CAM known as junctional adhesion molecule A (JAMA). Production of retro-proteins for R4 and JAMA allowed us to determine whether they preserved their original function, namely the binding of β-gal and recognition, respectively. This allowed us to study the structure-function relationship of retro-proteins from the IgSF. Here, we report the results of employing this retro-protein strategy for two examples of Ig domain-containing proteins.

Materials and Methods

Proteins and Plasmids

The anti-β-galactosidase ScFv Ab synthetic construct accession number was: GenBank CAA12398.1 (https://www.ncbi.nlm.nih.gov/protein/3090426). This sequence is also known as ScFv13. The amino acid sequences for ScFv13.R4 (i.e. R4) and retro R4. GLMS (glutamine-fructose-6-phosphate aminotransferase) has the accession number P17169, and its corresponding crystal structure is PDB ID 2J6H. The amino acid sequence for all proteins studied in this article. All plasmids hosting the proteins were pET28a and were Kanamycin resistant. Other proteins included β-galactosidase (Millipore Sigma, Burlington, Massachusetts, United States), anti-MBP mouse monoclonal Ab (catalog number E8032S, New England Biolabs, Massachusetts, United States), and anti-6xHis tag mouse monoclonal Ab (catalog number MA1-135, ThermoFisher Scientific, Massachusetts, United States).

Protein Expression and Purification

All proteins were expressed in Shuffle T7 Express competent *E. coli* (New England Biolabs). Growth media was composed of Terrific Broth solution I (24 g yeast extract, 12 g tryptone, and 4 mL 100% glycerol per L of ddH_2O) and Terrific Broth solution II (50 g capsule per L of ddH_2O, MP Biomedicals) supplemented with 100 μg/mL of Kanamycin. Protein expression was induced at an OD_{600} of 1 and with a final concentration of 0.25 mM IPTG (Apex Bioresearch, Genesee Scientific, El Cajon, California, USA). The temperature was lowered to 16°C and maintained for 18 h to promote proper protein folding. Protein purification was achieved with a standard buffer (50 mM Tris, pH 8, 500 mM NaCl), and membrane protein extraction was carried out using the same buffer supplemented with 5% CHAPS (AG Scientific, San Diego, California, United States). His-tagged proteins were purified according to the manufacturer's instructions for Ni-NTA resin (Prometheus Protein Biology, Genesee Scientific, El Cajon, California, United States). Amylose resin purification was carried out according to the manufacturer's recommendations (New England Biolabs, Massachusetts, United States).

Protein Modeling

Models and molecular graphic images were produced using the UCSF Chimera v.1.15 package from the Resource for Biocomputing, Visualization, and Informatics at the University of California, San Francisco (supported by NIH P41 RR-01081) [26].

Web-Based Analysis Tools

Ramachandran plots were obtained from the EMBL European Bioinformatics Institute (https://www.ebi.ac.uk/).

Enzyme-Linked Immunosorbent Assay (Elisa)

ELISA was used to evaluate the binding of purified R4 and rR4 to β-galactosidase (β-gal). ELISA plates were coated overnight at 4°C with 50 μL/well of β-gal in PBS (10 μg/mL). The plates were then blocked at room temperature for 2 h with 5% non-fat milk in PBS. Plate washing was accomplished using PBS supplemented with 0.1% Tween 20 (PBST). Purified R4 or rR4 samples were serially diluted in PBS containing 50 μg/mL BSA (PBS-BSA) and then added to the plates (100 μL/well). Plates were incubated for 1 h at room temperature and then washed with PBST. Horseradish peroxidase (HRP)-conjugated anti-6x-His Ab in PBS-BSA was added to the plates (50 μL/well). After 1 h of incubation at room temperature, plates were washed and then incubated with SigmaFast OPD HRP substrate (Millipore Sigma, Burlington, Massachusetts, United States) for 20 min. The reaction was quenched with H_2SO_4 and the absorbance of wells then measured at 490 nm. Equilibrium dissociation constants for wildtype R4 and rR4 were determined as described by Martineau [24]. The dissociation constant (K_d) for R4 and rR4 was derived from the absorbance data using Prism (GraphPad, Massachusetts, United States).

Mass Spectrometry Assay and Analysis

This analysis was performed at the Fritz B. Burns Biological Mass Spectrometry Facility, Brigham Young University, Provo, UT 84602. A typical protocol can be found in the literature [27].

Size Exclusion Chromatography

All size exclusion chromatography (SEC) was performed using the NGC Chromatography System and its accompanying software, Chro-

meLab (BioRad, Hercules, California, USA). The SEC column used to purify proteins of interest was ENrich™ SEC 650 10 × 300 (BioRad, Hercules, CA, USA). Protein concentration was determined using the Nanodrop Onec (ThermoFisher Scientific). PBS was employed as a running buffer for SEC. Fractions were pooled and concentrated as described above. The position of product peaks was compared to that of the size exclusion standards (BioRad, Catalog Number 151-1901).

Production of Outer Membrane Vesicles (OMVs)

The production of OMVs from Shuffle T7 express cells was performed according to a previous report by Prachayasittikul, et al. [28]. Briefly, 1 L of cultured *E. coli* typically yielded 5 g of cells. After centrifugation, the pellets were incubated with 50 mL of 100 mM EDTA, pH 8.0, for 1 h. Centrifugation at 15,000 g for 1 h removed unbroken cells. This was followed by ultracentrifugation at 100,000 g for 1 h to yield OMVs, which were then resuspended in PBS.

Cell Aggregation Assay Using Flow Cytometry (FC)

For this assay, the cell adhesion molecules JAMA or rJAMA were expressed in SHuffle T7 Express. At an OD_{600} of 1, cells were induced with 1 mM IPTG and shaken overnight at room temperature. After OD_{600} was reached, cells were diluted 1:5 in PBS and examined by FC. The assay for cell-adhesion molecule aggregation using FC protocols (iCLASP) was recently developed and published by our laboratory [29].

Analysis of Bacterial OMVs

OMV size and volume were confirmed by ZetaView (Particle Metrix, Ammersee, Germany). The settings used for reading the samples were as follows: laser wavelength: 488 nm; filter wavelength: scatter; sensitivity: 65; shutter: 150; cell temperature: 22°C; particles per frame: 35-140. All samples were prepared by sonication in a Branson 2800 ultrasonic water bath (Emerson Electric Co., St. Louis, Missouri, USA) for 30 seconds, followed by 1:250 dilution in Dulbecco's Phosphate-Buffered Saline (DPBS). The instrument was auto-aligned using an Applied Microspheres Nano Standards 100 nm polystyrene bead solution (Particle Metrix, Ammersee, Germany) diluted 1:500,000. All samples on the cell were scanned at 11 positions, with a minimum of 7 successful measurements.

Statistical Analysis

FC data (experimental slope) was analyzed using SAS software version 9 (SAS Institute Inc., Cary, NC, USA). The Mixed Procedure method was used to determine p-values, standard deviation, standard error, and statistical significance. For all experiments, $\alpha = 0.05$ was used. For each sample, data from four different experiments ($n = 4$) was collected, with each condition measured in 12 replicates. Thus, each data point corresponds to the average of 12 replicates and $n = 4$, or 48 data points. Statistically significant differences were investigated for all samples shown in each graph. The final analysis concluded that all treatments were statistically significant ($p < 0.01$), and significantly different from each other and the control. The t-test was employed for statistical analysis, with an asterisk representing a statistical significance between groups of four separate experiments and their standard deviation (SD).

Negative Staining Electron Microscopy of a Preparation of Shuffle t7 Express *E. Coli* omvs

Samples of OMVs were examined by transmission electron microscopy. The samples were placed on formvar-coated copper grids (Ted Pella Inc., Redding, California, USA) and allowed to rest for 2 min. Excess sample was removed using filter paper. After drying, the samples were negatively stained with a 0.3% aqueous solution of uranyl acetate (pH 4.0) and subsequently examined by scanning transmission electron microscopy (STEM) with a Thermo-Fisher Helios Nanolab 600 scanning electron microscope (Hillsborough, OR) operated at an accelerating voltage of 30 kV.

Results

Protein Sequences and Plasmids

ScFVs are a type of recombinant Ab consisting of ~25 kDa single polypeptides and containing the Ab variable light (VL) and variable heavy (VH) chains [30]. The two chains are connected by a flexible linker peptide made up of glycine and serine, with dispersed hydrophilic residues for increased solubility [31,32]. This is the approach typically used in previous work [33,34]. The amino acid sequence for R4 was obtained from the literature [24,25]. Full amino acid sequences for both R4 and retro-protein R4 (rR4). R4 and rR4 were subcloned into pET28a (kanamycin resistant) plasmid between NcoI and XhoI, leaving the 6xHis tag in frame. Figure 1 shows the basic characteristics of the R4 (1B) and rR4 (1C) structures (Figure 1A). Both proteins acquire the correct folding of IgSF members. Ramachandran plots for these modeled ScFv Abs revealed that rR4 has a similar secondary structure to that of R4, with some differences in the left-handed α-helix (Figure 1B,1C).

 DOI: 10.26717/BJSTR.2026.64.010079

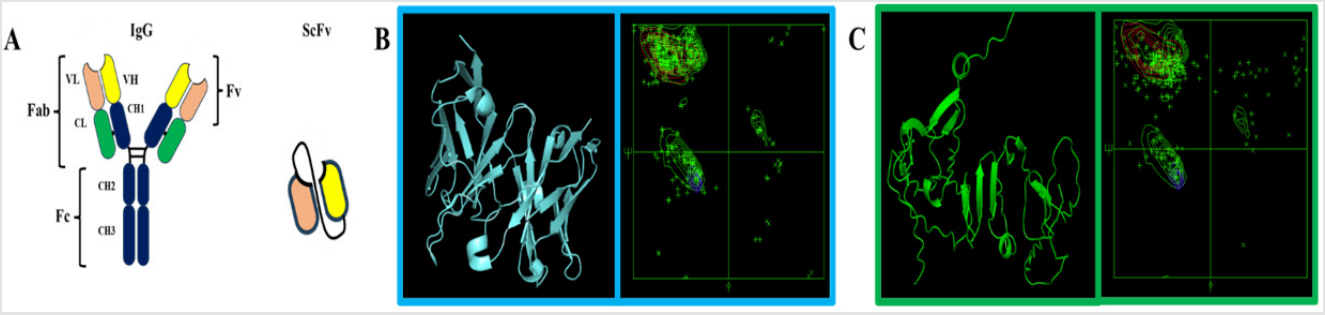

Figure 1: Basic structure of R4 and rR4.

A) Conceptual model of derived ScFv.

B) The structure of an ScFv (PDB ID 1BVK) is shown for schematic representation, with two domains and a typical Ramachandran plot.

C) The structure of rR4 generated with the UCSF Chimera v. 1.15 package shows the two protein domains and the Ramachandran plot.

Further characterization of ScFv R4 and rR4 was carried out using SEC. Figure 2A shows the different aggregation profiles for R4 and rR4. R4 elutes at its predicted size (29.5 kDa), whereas rR4 elutes in many aggregated states, in addition to its monomeric size. The rR4 SEC profile corresponds to a mixture of sizes between monomeric, dimeric, and largely aggregated. Under the peak at 10 mL, other proteins that contaminate the sample can be observed close to the 70 kDa mark (see also Figure 3).

This has been described previously for other targets of retro-protein design, where the expression and purification were unique and lower compared to the parent proteins [20]. The yield of R4 was 10-fold greater than that of rR4 per liter of *E. coli* culture.

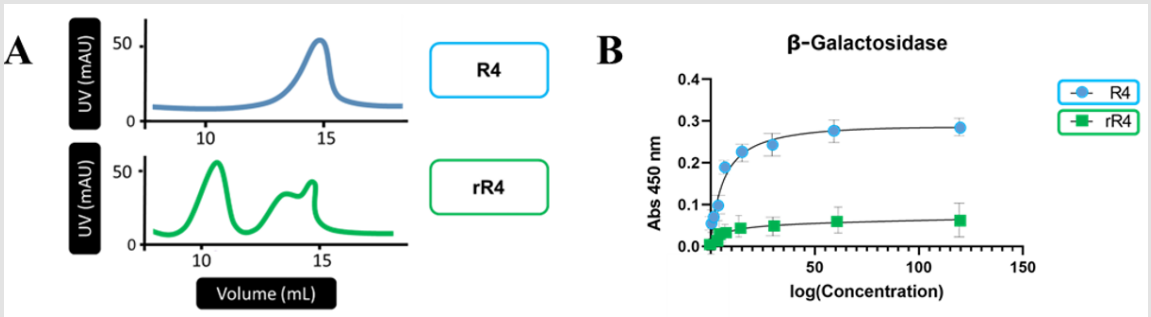

Figure 2: Size exclusion chromatography (SEC) purification profile for R4 and rR4, and ELISA.

A) The R4 SEC profile shows a monomer protein peak at about 15 mL, corresponding to a 30 kDa mass. The rR4 SEC profile retains monomeric properties similar to R4, but also displays other oligomeric properties.

B) Both R4 and rR4 were evaluated by ELISA against β-galactosidase (β-gal), the usual target of R4. The dissociation constant K_d for R4 and rR4 was derived from absorbance data using Prism (GraphPad, Massachusetts, USA). R4: K_d = 106.11±37 nM; rR4: K_d = 1737.82±207 nM.

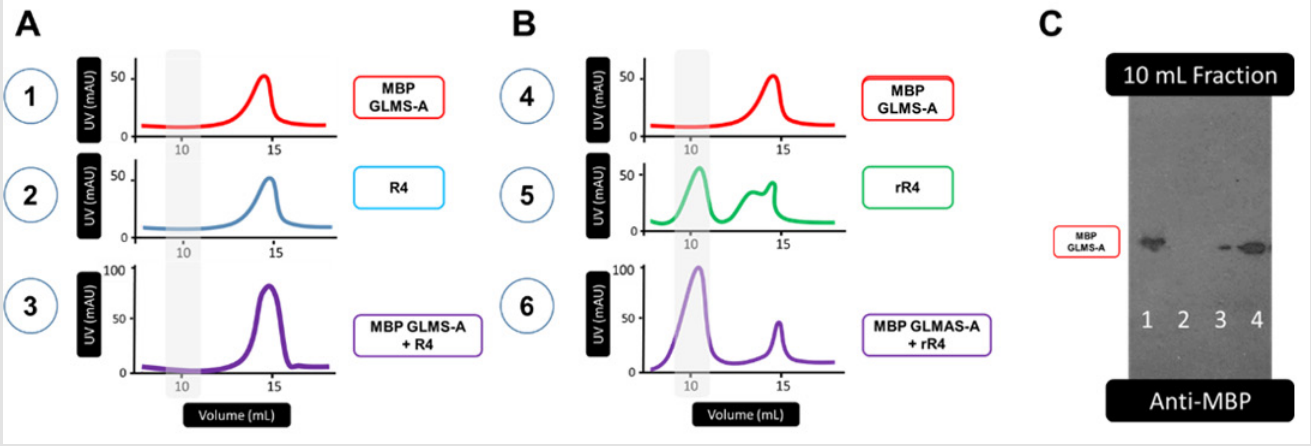

Figure 3: Comparison of SEC profiles of purified proteins and their mixture.

A) SEC of the individual proteins MBP_GLMS-A and R4, as well as a mixture of these purified proteins.

B) SEC of the individual proteins MBP_GLMS-A and rR4, as well as a mixture of these purified proteins.

C) Western blot using anti-MBP. Lane 1: purified MBP_GLMS-A as positive control; Lane 2: 10 ml SEC fraction of MBP GLMS-A (A.1); Lane 3: 10 ml SEC fraction of mixture R4 + MBP GLMS-A (A.3); Lane 4: 10 ml SEC fraction of mixture rR4 + MBP GLMS-A (B.6).

ELISA was performed on the monomeric forms of R4 and rR4 to determine binding to β-Gal, the usual target of R4. This is highly sensitive and specific method can detect and quantify specific protein interactions. As shown in Figure 2B, R4 clearly has strong affinity for β-Gal, whereas rR4 does not. This is illustrated by the Kd values, with the Kd quotient between rR4 and R4 being greater than 15-fold. The ELISA results showed that rR4 has a much lower affinity for β-Gal, and therefore its function differs from the parental R4 sequence.

Since the SEC profile of rR4 was clearly different to that of R4, we next purified both proteins in the absence of Imidazole in the washing steps. A concentration of 200 mM Imidazole (pH 8.0) was applied in the elution step. This strategy can help to determine if there are impurities in the purification process and identify new partners by subtracting the R4 profile from the rR4 profile. Purified proteins were loaded and separated on a gel, and then detected by Coomassie staining as shown in Figure 4A. A protein of approximately 70 kDa in size contaminates the rR4 eluate, but the same band was not present in NiNTA-purified R4 (Figure 4B). Thus, our strategy enabled the identification of another property of rR4 that distinguishes it from R4.

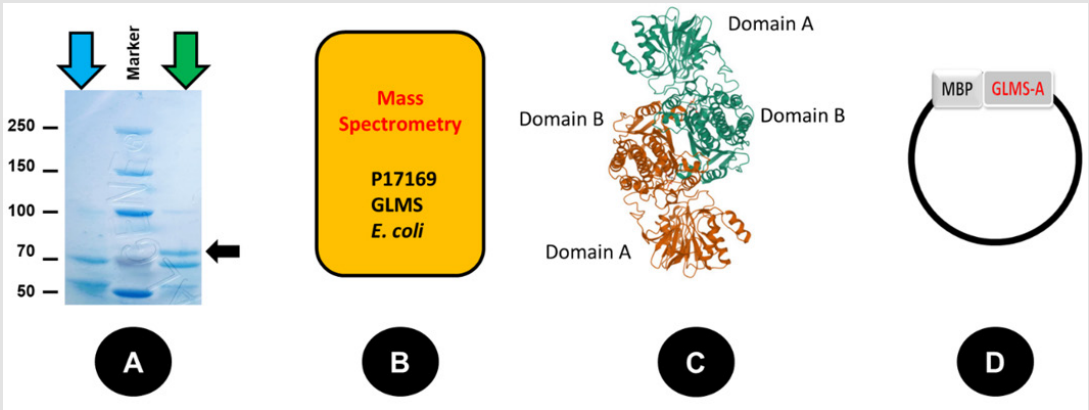

Figure 4: Identification of the binding partner for rR4. Validation of R4 and rR4 by SDS-PAGE and Mass Spectrometry.

A) SDS PAGE shows that R4 (light blue arrow) and rR4 (green arrow) share the same molecular weight of 30 kDa. Additionally, purification of rR4 with NiNTA resin results in the co-elution of another protein (black arrow) that is absent from the R4 purification. The middle lane shows molecular weight markers.

B) Mass Spectrometry identified the additional protein as glucosamine-6-phosphate synthase (GLMS), protein accession number P17169.

C) The crystal structure of GLMS (PDB ID 1JXA) shows a homodimer between the B domains.

D) The plasmid construct for the study of GLMS and rR4 interactions is a fusion protein between MBP and domain A of GLMS (Figure 1S).

The newly discovered protein was examined by Mass Spectrometry (data in Supplementary files) and identified as glucosamine-6-phosphate synthase (GLMS). The crystal structure of GLMS is shown in Figure 4C. Assessment of the GLMS quaternary organization (dimer) from its crystal structure allows its relationship with rR4 to be determined. This structure depicts two domains, A and B, with the formation of a dimer (monomers are green and orange) through the B domain. Since the B domain will lead to self-association of GLMS, we created a maltose binding protein (MBP) fusion and GLMS-A domain. This strategy produces a monomeric molecule that can be studied by SEC in relation to mobility, and to changes in aggregation in the presence of rR4. Figure 4D, represents a plasmid with the intended fusion MBP_GLMS-A. GLMS-A was cloned into the pMALc2x plasmid to generate MBP_GLMS-A. SEC and Western blot analysis of the resulting proteins was subsequently performed. Figure 3A.1 shows the SEC profiles for R4, MBP_GLMS-A (Figure 3A.2), and the mixture of both proteins (Figure 3A.3). Single proteins eluted at a monomeric size, while the mixture of both proteins eluted as an overlapping peak of the monomeric sizes. Figure 3B shows the SEC profiles for rR4 (Figure 3B.4), MBP_GLMS-A (Figure 3B.5), and the mixture of both proteins (Figure 3B.6). As expected, MBP_GLMS-A elutes as a monomeric size, whereas rR4 elutes as a mixture of monomeric and aggregated forms. The mixture of rR4 and MBP_GLMS-A shifted to an elution volume that indicated an interaction between proteins.

To verify that MBP_GLMS-A did indeed interact with rR4, Western blot with anti-MBP Ab (1:50,000) was performed (Figure 3C). The results showed that MBP_GLMS-A was associated with rR4, but not with R4 or as a self-aggregate. We therefore inferred from this experiment that rR4 performs a similar function to R4 as an Ab only, but with its affinity directed towards a different target, GLMS. Having noted the conservation of function of rR4 with regard to binding or recognition, albeit with a different target than R4, we next studied whether function was also preserved for the retro-protein of another member of the IgSF, junctional adhesion molecule A (JAMA). JAMA normally functions as a CAM, specifically in cell-cell interactions [35]. CAMs of the IgSF regulate important processes such as cell proliferation, differentiation and morphogenesis. JAMA is an IgSF CAM with no catalytic activity, but is nevertheless involved in a variety of biological processes. We recently presented evidence that JAMA is calcium sensitive [36] and that its aggregation can be triggered by different cations, especially by zinc [37]. We prepared pET28a plasmids for the expression of JAMA and rJAMA in *E. coli*. To observe the cell-cell interactions driven by CAMs, we fused these proteins to outer membrane protein W (OmpW). This native membrane protein of *E. coli* is found exclusively in the outer membrane. The OmpW-JAMA and OmpW-rJAMA sequences.

Due to the difficulties in working with membrane proteins and the inevitable use of detergents, we created MBP fusion proteins with the soluble domains of JAMA and rJAMA to study aggregation. JAMA mediates cell-cell interactions in the tight junction of endothelial and epithelial cells through homotypic interactions between this protein in adjacent cells [38]. SEC profiles for the JAMA and rJAMA soluble domains in solution are shown in Figure 5A. JAMA is expected to behave mostly as a monomer in the absence of environmental factors present at the tight junction. Here, it would normally form dimers and other levels of aggregation in the presence of cations, with zinc influencing JAMA to form larger than 10-mer aggregation units [36-38]. A stark contrast between monomeric JAMA and multimeric rJAMA is evident in the SEC profiles (Figure 5A). The elution volumes suggest that rJAMA has a molecular weight of > 500 kDa. JAMA aggregation is believed to occur in a trans orientation between JAMA molecules present in opposite or neighboring cells [38]. To determine if rJAMA also has the ability to form trans interactions and thus drive cell-cell interactions, we expressed full-length JAMA or rJAMA on the surface of *E. coli*. This was carried out using our recently published strategy and methodology for expressing CAMs on the outer membrane of *E. coli* [29,39].

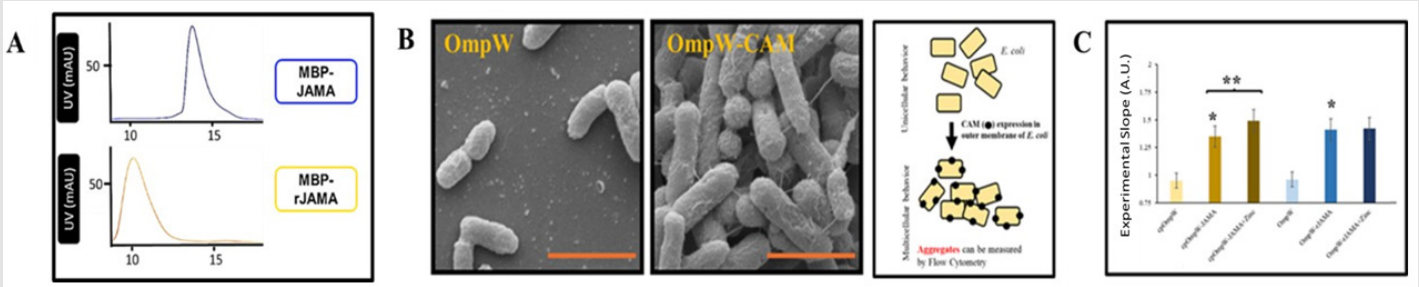

Figure 5: Expression of JAMA and rJAMA in *E. coli*.

A) The MBP-JAMA SEC profile shows a monomeric peak at 16 mL volume and with a predicted size of 70 kDa. The MBP-rJAMA SEC profile is shifted to a higher order of aggregation, with a predicted size of > 500 kDa.

B) *E. coli* expressing outer membrane protein W (OmpW) retain unicellular behavior, whereas OmpW-CAMs change the phenotype to multicellular aggregates. The orange bar represents 2 µm. The panel to the right of the pictures represents a model of the technique.

C) Cell aggregation can be determine by Flow Cytometry [29]. This technique is referred to as iCLASP and determines the slope for all cells moving through the detector and recorded by size. A greater slope corresponds to more aggregation. The graph plots the Experimental Slope in arbitrary units for cells expressing OmpW only, as well as for the test CAMs.

The method is referred to as iCLASP and uses FC protocols to determine the extent of aggregation of bacteria expressing CAMs. Figure 5B is a visual demonstration of the unicellular behavior of E. coli in the absence of CAMs (left panel), and the aggregation induced by CAM overexpression (middle panel). Figure 5C shows that both JAMA and rJAMA induce aggregation at levels above those of the control (no CAM expression). JAMA was also observed to respond to the presence of zinc by further aggregation, whereas rJAMA did not display this behavior. This was anticipated in view of previous experiments showing that JAMA is a monomer, whereas rJAMA is already an oligomer. Hence the results indicate that rJAMA mediates cell-cell interactions, corresponding to trans interactions. Following the observation that rR4 has affinity for a new target, GLMS, a pull-down experiment was performed using recombinant MBP-JAMA and MBP-rJAMA attached to the Amylose resin, thus allowing purification of MBP-fusions [40]. As shown in Figure 6, JAMA has affinity for JAMA, but not for rJAMA, and vice versa (Figure 6A, 6B). The final experimental design employed a known technique to extract outer membrane vesicles (OMVs) from bacteria using EDTA [28]. Cells expressing OmpW alone (labeled as OMV) or OmpW fusions with JAMA or rJAMA (labeled as OMV JAMA and OMV rJAMA, respectively) were examined by qualitative and quantitative methods. Figure 7A shows qualitative electron microscopy images of OMV, OMV JAMA and OMV rJAMA in the presence of buffer (PBS) or zinc.

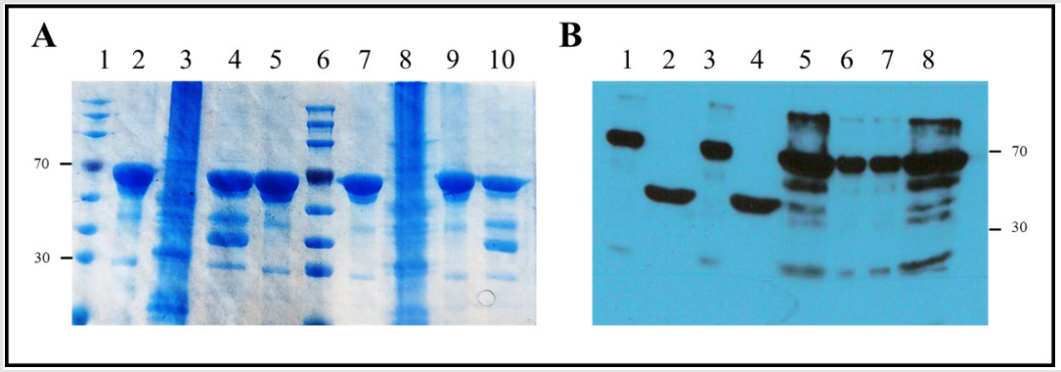

Figure 6: Characterization of JAMA and rJAMA homotypic interactions.

A) Pull-down of OmpW-JAMA or rJAM by MBP fused to the corresponding soluble domains. Lane 1: Molecular weight markers; Lane 2: MBP-JAMA; Lane 3: detergent lysate OmpW-JAMA; Lane 4: pull-down of OmpW-JAMA with MBP-JAMA; Lane 5: pull-down of OmpW-JAMA with MBP-rJAMA; Lane 6: molecular weight markers; Lane 7: MBP-rJAMA; Lane 8: detergent lysate OmpW-rJAMA; Lane 9: pull-down of OmpW-rJAMA with MBP-JAMA; Lane 10: pull-down of OmpW-JAMA with MBP-rJAMA.

B) Western blot with anti-6xHis tag. Lane 1: MBP-JAMA; Lane 2: lysate OmpW-JAMA; Lane 3: MBP-rJAMA; Lane 4: Lysate OmpW-rJAMA; Lane 5: pull-down of OmpW-JAMA with MBP-JAMA; Lane 6: pull-down of OmpW-rJAMA with MBP-JAMA; Lane 7: pull-down of OmpW-JAMA with MBP-rJAMA; Lane 8: pull-down of OmpW-rJAMA with MBP-rJAMA.

As expected, OMV and OMV rJAMA did not form any aggregates in the presence of zinc. However, OMV JAMA formed larger aggregates in the presence of zinc, as expected. Figure 7B and Figure 7C show quantitative results obtained using ZetaView [41]. An alternative approach to the analysis of OMV size and volumetric characteristics is through the application of single particle interferometric reflectance imaging sensing (SP-IRIS) [42]. ZetaView is a nanoparticle tracking analysis (NTA) instrument that measures hydrodynamic particle size and volume, as well as concentration and fluorescence [41]. Figure 7B shows the volume of OMVs isolated from different *E. coli* cells expressing the above-mentioned proteins. OMV JAMA and OMV rJAMA had significantly larger volumes than OMV alone. Finally, OMV JAMA in the presence of zinc displayed a significantly larger volume compared to OMV JAMA in PBS only. This was not observed with OMV rJAMA. Figure 7C shows the recordings obtained during experimentation and which are a qualitative representation of the data presented in Figure 7B. Original images can be found in the Supplementary materials.

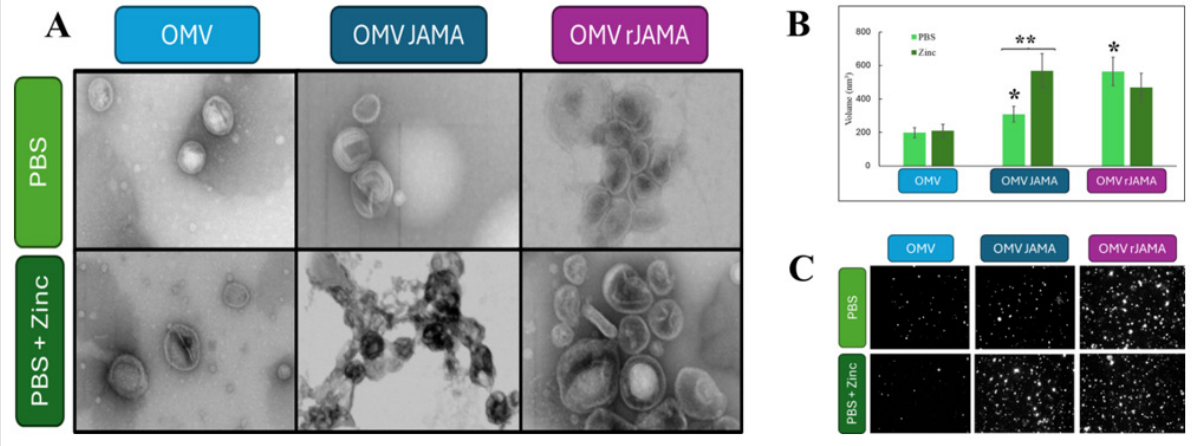

Figure 7: Characterization of outer membrane vesicles (OMVs) from *E. coli* expressing JAMA or rJAMA.

A) Electron microscopy imaging of OMVs from cells expressing OmpW, OmpW-JAMA, or OmpW-rJAMA. OMVs were subjected to PBS, or to PBS + 2 mM ZnCl2.

B) Characterization of OMV volume using ZetaView under the same conditions as described in panel A. * indicates $p<0.05$ for the sample vs. OMV. ** indicates $p<0.05$ for JAMA vs. JAMA in the presence of zinc.

C) Visual representation of the results shown in panel B and obtained using ZetaView software.

Discussion

The literature on retro-proteins is currently limited to a handful of cases. As stated previously, the lack of native retro-proteins means that non-natural retro-proteins must be designed and engineered. Past studies of retro-proteins have focused mainly on peptides and alpha helical proteins. Peptidomimetics that are effective at modulating protein-protein interactions while also being resistant to proteolysis have potential therapeutic applications. Due to underperformance, one peptidomimetic strategy is to employ D-amino acids and reverse sequences in order to mimic a lead peptide conformation, either separately or as the combined retro-inverso peptide. In 2013, Atzori, et al. [43] applied this strategy to examine the conformations of inverse, reverse and retro-inverso peptides of p53(15–29) using implicit solvent molecular dynamics simulation and circular dichroism spectroscopy. They concluded that retro-inverso peptides had disadvantages as mimics, and further chemical modification was required before this concept could be used in peptidomimetic design. Other workers concluded that reversing the sequence of amino acids structured as a β-sheet retained this structural property, but impacted the peptide's molecular surface behavior [44]. The folding of retro-protein A, originating from the retro-sequence of the B domain of Staphylococcal protein A, was studied two decades ago [21].

Retro-protein A also forms a three-helix bundle structure in solution, thus preserving the topology of native protein A. However, two main structural aspects were highlighted in the conclusion to this work: secondary structure elements in the retro-protein do not exactly match their counterparts in the original protein structure, and the amino acid side chain contact pattern of the hydrophobic core is partly conserved [21]. Retro-proteins obtained from backward reading of the SH3 sequence, a 61-residue protein that folds as a five-stranded orthogonal β-sheet sandwich, were engineered and expressed in *E. coli* [20]. Expression yields were insufficient to allow purification and further structural characterization of the retro-protein [20]. However, after applying Far-UV Circular Dichroism analysis and temperature scans, Lacroix and colleagues concluded that retro-SH3 could be unfolded [20]. A recent study found the retro-inverso strategy works poorly for molecular mimicry of biologically active helical peptides [45]. More positive reports of retro-inverso strategies have described a Urokinase receptor antagonist for the treatment of metastatic sarcoma [46], antimicrobial peptides [47], a solubilizing fusion tag [48], and a retro-inverso collagen modulator peptide with enhanced stability and activity in vitro [49]. In the present work we attempted to study retro-proteins containing Ig domains, ScFv and JAMA. Similar to previous reports in the literature, we were confronted with solubility issues and lower yields, especially for rR4 (data not shown). Nevertheless, we did not encounter a loss of folding, as reported by others [20].

This was determined by identifying the functional activity of both rR4 and rJAMA. The primary structure of a protein determines its three-dimensional structure, or fold, which in turn influences its function [50]. This is known as the sequence-structure-function paradigm. Proteins with similar amino acid sequences often perform similar biochemical functions, even if they are from distantly related organisms. Thus, function can be identified based on protein homology and structural properties. As suggested in the literature, retro- or retro-inverso proteins have an identical amino acid composition. However, the primary structure and the order in which these amino

acids are synthesized and react chemically and biophysically to the environment as a new unit are completely different. Our experiments found that rR4 folding showed strong similarity to R4, as revealed by comparison of the Ramachandran plots (Figure 1). Nevertheless, in the absence of proper crystal structures, the models used to generate the plots may be influenced by our ability to predict secondary and tertiary structures of proteins. The folding of proteins occurs in part due to clashes between amino acids and the hydrophobicity profiles of those amino acids. In any event, the emergence of function indicates that rR4 and rJAMA can be folded based on their respective primary sequence. As discussed above, native retro-proteins have yet to be reported. Moreover, aside from some retro-inverso peptides, functional retro-proteins have not been identified or characterized.

CAMs perform a wide range of functions at cell contact areas. These include mechanical support, target recognition, differentiation and specialization of membrane microdomains, and the initiation, organization and regulation of signaling platforms. The largest protein family among CAMs is the IgSF [5,9,10]. The present study showed that in spite of low yields, rR4 retains its ability for target recognition. R4 is an ScFv that specifically targets β-Gal. Although that property was lost in rR4, Mass Spectrometry revealed that GLMS was the target for rR4. Because GLMS is a native *E. coli* protein and contamination is a constant concern, we did not complete the analysis with an ELISA.

In the case of JAMA, rJAMA retained its ability to perform cell-cell interactions through self-assembly of its extracellular domain. We characterized the aggregation profile of JAMA and rJAMA, and determined that rJAMA forms large aggregates that deviate from the behavior of JAMA in solution. As membrane proteins, both JAMA and rJAMA drive cell-cell interactions with similar phenotypic consequences in *E. coli*. The whole cell aggregation of *E. coli*. was characterized by iCLASP quantitative methodology, but this could not be used to quantify differences in cell behavior. We therefore extracted OMVs from cells expressing JAMA or rJAMA. This strategy also bypasses the reduced yields for soluble retro-proteins. Differences could also arise due to the different chaperones that aid protein folding when the target is soluble, or membrane bound [51-54]. Characterization of OMVs revealed that the behavior of soluble JAMA and rJAMA was replicated.

OMV JAMA showed lesser ability to aggregate OMVs, while cell-cell interactions (OMV-OMV) were enhanced in the presence of zinc (Figure 7). In contrast to JAMA, rJAMA showed a superior ability to cause OMV-OMV interactions. rJAMA also demonstrated insensitivity to zinc (Figure 7), and correlated with the SEC profile of soluble rJAMA (Figure 5). The ZetaView nanoparticle tracker is a very useful tool for the qualitative and quantitative characterization of OMVs (Figure 7B & 7C). We previously used SEC to qualitatively characterize soluble JAMA and rJAMA. Because rJAMA was already aggregated beyond the SEC sensitivity, the effect of zinc could not be confirmed. The susceptibility of JAMA to zinc was previously reported by our group [37]. We have now confirmed using ZetaView that aggregation by rJAMA is not dependent on zinc. Our experimental design and performance provided evidence that Ig domain-containing proteins can be converted to retro-proteins. Although the yields are low and thus challenging to work with, the function of these new primary sequences is retained and is similar to known functions of the parental protein. The challenge, as revealed by rR4, is to identify the new targets for these retro-ScFvs. When the amino acid sequences of rR4 and rJAMA were entered into the BLAST tool, the results obtained were "No significant similarity found", thereby confirming the unique sequence of these retro-proteins. They have perhaps never existed in nature before, and therefore not be required to fold. This may be another indication that retro-native proteins do not exist.

The problem of folding these proteins could be solved by enhancing the chaperone battery present in a cell, e.g. GroEL [55]. The use of fusion proteins such as MBP can also help to increase yields [56]. We found that R4 yields were 10-fold higher than those of rR4, while MBP-JAMA was expressed 3-4-fold more than MBP-rJAMA. These approaches can overcome the unfavorable crowding of amino acids in retro-proteins, as well as long sequences of amino acids in orders that have never been synthesized. Amino acid residues have a chiral center, and reversing the sequence could alter the structure of the peptide and eventually change or modify its function, as observed with rR4. Retro-proteins can modify other properties, such as lateral conductivity (conductivity on the surface of water using Langmuir monolayer), even when the hydrophobicity and sequence length is the same [57]. It remains to be determined whether these proteins are less susceptible to proteases.

Conclusion

The findings from this study are compelling in terms of revealing how the peptide primary structure plays an essential role in dictating specific surface activity for molecules with a similar secondary structure (Ig domain, β-sheet) and identical hydrophobic profiles. Based on our results, R4 and JAMA are appropriate templates for the generation of retro-proteins. Preparing retro-proteins of Ig-domain (β-sheet)-containing proteins appears to be more successful than retro-peptides, or retro-proteins with an α-helical nature. This work provides both qualitative and quantitative evidence that retro-proteins can retain function while changing specificity. Our findings could inform future work on peptidomimetics or on the design of therapeutics. Currently, Ab libraries generated by DNA recombination have monopolized efforts for the discovery of Abs with therapeutic capabilities. The Ab market is growing due to the increasing prevalence of chronic diseases, advances in biotechnology, and the COVID-19 pandemic. The North American market for Ab drugs is expected to grow from $132.2 billion in 2024 and reach $225 billion by the end of 2030. The global monoclonal Ab market size was estimated at USD 230 billion in 2023 and is expected to increase to around USD 680 billion by 2035. The current study identified a key aspect of Ig-domain-containing retro-proteins, namely that their function is preserved. This is the first step in understanding how these retro-proteins can be adapted for the discovery of Abs against targets with therapeutic value.

As stated in the Introduction, no native retro-proteins have yet been reported. Nevertheless, we have provided evidence for the functionality and potential application of retro-proteins. DNA libraries employed in the search for new Abs have theoretical library size of 10^{80}, with current libraries may contain up to 10^{12} Abs (https://www.youtube.com/watch?v=RziWVws21Is&t=969s). The large libraries may miss retro-sequences that could be of great value. Additionally, a library of retro-sequences may indicate Abs with low stability or solubility. Future work should focus on the structure, solubility and stability optimization of retro-proteins. At the fundamental level, a better understanding of why retro-proteins do not exist in nature may also be of great value in generating Abs libraries for discovery.

References

1. Adhav V A, K Saikrishnan (2023) The Realm of Unconventional Noncovalent Interactions in Proteins: Their Significance in Structure and Function. ACS Omega 8(25): 22268-22284.
2. Anfinsen C B (1973) Principles that govern the folding of protein chains. Science 181(4096): 223-230.
3. Iorgulescu J B (2023) Reporting of Immunotherapy and Biologic Therapy in the National Cancer Database. JAMA Oncol 9(7): 1003.
4. Saeed A F, Rongzhi Wang, Sumei Ling, Shihua Wang (2017) Antibody Engineering for Pursuing a Healthier Future. Front Microbiol 8: 495.
5. Aricescu A R, E Y Jones (2007) Immunoglobulin superfamily cell adhesion molecules: zippers and signals. Curr Opin Cell Biol 19(5): 543-550.
6. Berezin V A, P S Walmod (2014) Cell adhesion molecules: implications in neurological diseases. Advances in neurobiology. New York: Springer, pp. 410
7. Alejandra W P, Jiménez Pérez Miriam Irene, Gonzalez Sanchez Fabio Antonio, Rojo Gutierrez Rocio Patricia, Torres Anguiano Elizabeth, et al. (2023) Production of monoclonal antibodies for therapeutic purposes: A review. Int Immunopharmacol 120: 110376.
8. Elgundi Z, Mouhamad Reslan, Esteban Cruz, Vicki Sifniotis, Veysel Kayser (2017) The state-of-play and future of antibody therapeutics. Adv Drug Deliv Rev 122: 2-19.
9. Janeway C (2001) Immunobiology: The Immune System in Health and Disease.: Garland Pub.
10. Williams A F, A N Barclay (1988) The immunoglobulin superfamily--domains for cell surface recognition. Annu Rev Immunol 6: 381-405.
11. Bemani P, M Mohammadi, A Hakakian (2018) ScFv Improvement Approaches. Protein Pept Lett 25(3): 222-229.
12. Silva T A, Rodrigo Barbosa Aguiar, Marcelo Mori, Gabriel Esquitini Machado, Barbara Hamaguchi, et al. (2023) Potential of an anti-bevacizumab idiotype scFv DNA-based immunization to elicit VEGF-binding antibody response. Gene Ther 30(7-8): 598-602.
13. Dreier B, A Pluckthun (2018) Rapid Selection of High-Affinity Antibody scFv Fragments Using Ribosome Display. Methods Mol Biol 1827: 235-268.
14. Zhang S, L Wu, M Dang (2024) Antibody mimetics: The next generation antibody engineering, a retrospective and prospective analysis. Biotechnol J 19(1): e2300532.
15. Keri D, Matt Walker, Isha Singh, Kyle Nishikawa, Fernando Garces (2024) Next generation of multispecific antibody engineering. Antib Ther 7(1): 37-52.
16. Qerqez A N, R P Silva, J A Maynard (2023) Outsmarting Pathogens with Antibody Engineering. Annu Rev Chem Biomol Eng 14: 217-241.
17. Tsuchikama K, Yasuaki Anami, Summer Y Y Ha, Chisato M Yamazaki (2024) Exploring the next generation of antibody-drug conjugates. Nat Rev Clin Oncol 21(3): 203-223.
18. Guichard G, N Benkirane, G Zeder Lutz, M H van Regenmortel, J P Briand, et al. (1994) Antigenic mimicry of natural L-peptides with retro-inverso-peptidomimetics. Proc Natl Acad Sci U S A 91(21): 9765-9769.
19. Chorev M, M Goodman (1995) Recent developments in retro peptides and proteins--an ongoing topochemical exploration. Trends Biotechnol 13(10): 438-445.
20. Lacroix E, A R Viguera, L Serrano (1998) Reading protein sequences backwards. Fold Des 3(2): 79-85.
21. Olszewski K A, A Kolinski, J Skolnick (1996) Does a backwardly read protein sequence have a unique native state? Protein Eng 9(1): 5-14.
22. Mittl P R, C Deillon, D Sargent, N Liu, S Klauser, et al. (2000) The retro-GCN4 leucine zipper sequence forms a stable three-dimensional structure. Proc Natl Acad Sci U S A 97(6): 2562-2566.
23. Jumper J, Richard Evans, Alexander Pritzel, Tim Green, Michael Figurnov, et al. (2021) Highly accurate protein structure prediction with AlphaFold. Nature 596(7873): 583-589.
24. Martineau P, P Jones, G Winter (1998) Expression of an antibody fragment at high levels in the bacterial cytoplasm. J Mol Biol 280(1): 117-127.
25. Karlsson A J, Hyung Kwon Lim, Hansen Xu, Mark A Rocco, Matthew A Bratkowski, et al. (2012) Engineering antibody fitness and function using membrane-anchored display of correctly folded proteins. J Mol Biol 416(1): 94-107.
26. Pettersen E F, Thomas D Goddard, Conrad C Huang, Gregory S Couch, Daniel M Greenblatt, et al. (2004) UCSF Chimera--a visualization system for exploratory research and analysis. J Comput Chem 25(13): 1605-1612.
27. Goldman A R, Lynn A Beer, Hsin Yao Tang, Peter Hembach, Delaine Zayas Bazan, et al. (2019) Proteome Analysis Using Gel-LC-MS/MS. Curr Protoc Protein Sci 96(1): e93.
28. Prachayasittikul V, Chartchalerm Isarankura Na Ayudhya, Tanawut Tantimongcolwat, Chanin Nantasenamat, Hans Joachim Galla (2007) EDTA-induced membrane fluidization and destabilization: biophysical studies on artificial lipid membranes. Acta Biochim Biophys Sin (Shanghai) 39(11): 901-913.
29. Rollins J, Tyler Worthington, Allison Dransfield, Jordan Whitney, Jordan Stanford, et al. (2023) Expression of Cell-Adhesion Molecules in *E. coli*: A High Throughput Screening to Identify Paracellular Modulators. Int J Mol Sci 24(12): 9784.
30. Worn A, A Pluckthun (1998) An intrinsically stable antibody scFv fragment can tolerate the loss of both disulfide bonds and fold correctly. FEBS Lett 427(3): 357-361.
31. Tassew N G, Jason Charish, Larisa Chestopalova, Philippe P Monnier (2009) Sustained *in vivo* inhibition of protein domains using single-chain Fv recombinant antibodies and its application to dissect RGMa activity on axonal outgrowth. J Neurosci 29(4): 1126-1131.
32. Boldicke T (2017) Single domain antibodies for the knockdown of cytosolic and nuclear proteins. Protein Sci 26(5): 925-945.
33. de Aguiar R B, Tábata de Almeida da Silva, Bruno Andrade Costa, Marcelo Ferreira Marcondes Machado, Renata Yoshiko Yamada, et al. (2021) Generation and functional characterization of a single-chain variable fragment (scFv) of the anti-FGF2 3F12E7 monoclonal antibody. Sci Rep 11(1): 1432.
34. Ahmad Z A, Swee Keong Yeap, Abdul Manaf Ali, Wan Yong Ho, Noorjahan

Banu Mohamed Alitheen, et al. (2012) scFv antibody: principles and clinical application. Clin Dev Immunol 2012: 980250.

35. Steinbacher T, D Kummer, K Ebnet (2018) Junctional adhesion molecule-A: functional diversity through molecular promiscuity. Cell Mol Life Sci 75(8): 1393-1409.
36. Mendoza C, Sai Harsha Nagidi, Kjetil Collett, Jacob Mckell, Dario Mizrachi (2022) Calcium regulates the interplay between the tight junction and epithelial adherens junction at the plasma membrane. FEBS Lett 596(2): 219-231.
37. Mendoza C N S H, Peterson K, Mizrachi D (2022) Cations as Molecular Switches for Junctional Adhesion Molecule-A. Biomedical Journal of Scientific & Technical Research 42(3): 33558-33570.
38. Ebnet K (2017) Junctional Adhesion Molecules (JAMs): Cell Adhesion Receptors with Pleiotropic Functions in Cell Physiology and Development. Physiol Rev 97(4): 1529-1554.
39. Rollins J, Tyler Worthington, Allison Dransfield, Jordan Whitney, Jordan Stanford, et al. (2021) Expression of cell-adhesion molecules in *E. coli*: a high-throughput method to identify paracellular modulators. Cold Spring Harbor Laboratory 24(12): 9784.
40. Duong Ly K C, S B Gabelli (2015) Affinity Purification of a Recombinant Protein Expressed as a Fusion with the Maltose-Binding Protein (MBP) Tag. Methods Enzymol 559: 17-26.
41. Bachurski D, Maximiliane Schuldner, Phuong Hien Nguyen, Alexandra Malz, Katrin S Reiners, et al. (2019) Extracellular vesicle measurements with nanoparticle tracking analysis - An accuracy and repeatability comparison between NanoSight NS300 and ZetaView. J Extracell Vesicles 8(1): 1596016.
42. Daaboul G G, Paola Gagni, Luisa Benussi, Paolo Bettotti, Miriam Ciani, et al. (2016) Digital Detection of Exosomes by Interferometric Imaging. Sci Rep 6: 37246.
43. Atzori A, Audrey E Baker, Mark Chiu, Richard A Bryce, Pascal Bonnet (2013) Effect of sequence and stereochemistry reversal on p53 peptide mimicry. PLoS One 8(7): e68723.
44. Ambroggio E E, Benjamín Caruso, Marcos A Villarreal, Vincent Raussens, Gerardo D Fidelio (2016) Reversing the peptide sequence impacts on molecular surface behaviour. Colloids Surf B Biointerfaces 139: 25-32.
45. Li C, Marzena Pazgier, Jing Li, Changqing Li, Min Liu, et al. (2010) Limitations of peptide retro-inverso isomerization in molecular mimicry. J Biol Chem 285(25): 19572-19581.
46. Carriero M V, Katia Bifulco, Vincenzo Ingangi, Susan Costantini, Giovanni Botti, et al. (2017) Retro-inverso Urokinase Receptor Antagonists for the Treatment of Metastatic Sarcomas. Sci Rep 7(1): 1312.
47. Franco O L (2022) Development of antimicrobial peptides as a strategy for infectious disease control. Peptides 150: 170761.
48. Xie X, Pei Wu, Xiaochen Huang, WenFeng Bai, Bowen Li, et al. (2022) Retro-protein XXA is a remarkable solubilizing fusion tag for inclusion bodies. Microb Cell Fact 21(1): 51.
49. Errante F, Marco Pallecchi, Gianluca Bartolucci, Elena Frediani, Francesca Margheri, et al. (2024) Retro-Inverso Collagen Modulator Peptide Derived from Serpin A1 with Enhanced Stability and Activity *In Vitro*. J Med Chem 67(6): 5053-5063.
50. Sercinoglu O, P Ozbek (2020) Sequence-structure-function relationships in class I MHC: A local frustration perspective. PLoS One 15(5): e0232849.
51. Pfanner N (1999) Who chaperones nascent chains in bacteria? Curr Biol 9(19): R720-R724.
52. Lill R, E Crooke, B Guthrie, W Wickner (1988) The "trigger factor cycle" includes ribosomes, presecretory proteins, and the plasma membrane. Cell 54(7): 1013-1018.
53. He W, Gangjin Yu, Tianpeng Li, Ling Bai, Yuanyuan Yang, et al. (2021) Chaperone Spy Protects Outer Membrane Proteins from Folding Stress via Dynamic Complex Formation. mBio12(5): e0213021.
54. Castanie Cornet M P, N Bruel, P Genevaux (2014) Chaperone networking facilitates protein targeting to the bacterial cytoplasmic membrane. Biochim Biophys Acta 1843(8): 1442-1456.
55. Marchenkov V V, G V Semisotnov (2009) GroEL-assisted protein folding: does it occur within the chaperonin inner cavity? Int J Mol Sci 10(5): 2066-2083.
56. Raran Kurussi S, K Keefe, D S Waugh (2015) Positional effects of fusion partners on the yield and solubility of MBP fusion proteins. Protein Expr Purif 110: 159-164.
57. Alvarez A B, Marcelo Pino, Steffen B Petersen, Gerardo Daniel Fidelio (2021) Stitching together a nm thick peptide-based semiconductor sheet using UV light. Colloids Surf B Biointerfaces 203: 111734.

ISSN: 2574-1241

DOI: 10.26717/BJSTR.2026.64.010079

Dario Mizrachi. Biomed J Sci & Tech Res

Submission Link: https://biomedres.us/submit-manuscript.php